Pergamon

PII: S0042-6989(96)00133-2

Vision Res., Vol. 36, No. 24, pp. 3955–3967, 1996

Printed in Great Britain
0042-6989/96 $15.00 + 0.00

Spatial and Temporal Properties of Cat Horizontal Cells after Prolonged Dark Adaptation

M. J. M. LANKHEET,*† M. H. ROWE,* R. J. A. VAN WEZEL,* W. A. van de GRIND*

We studied the change of spatial and temporal response properties for cat horizontal (H-) cells during prolonged dark adaptation. H-cell responses were recorded intracellularly in the optically intact, *in vivo* eye. Spatial and temporal properties were first measured for light-adapted H-cells, followed by a period of dark adaptation, after which the same measurements were repeated. During dark adaptation threshold sensitivity was measured at regular intervals. Stable, long lasting recordings allowed us to measure changes of sensitivity and receptive field characteristics for adaptation periods up to 45 min. Although cat H-cells showed no signs of dark suppression or light sensitization, they remained insensitive in the scotopic range, even after prolonged dark adaptation. Absolute thresholds were in the low mesopic range. The sensitization was brought about by a shift from cone to rod input, and by substantial increases of both spatial and temporal integration upon dark adaptation. The length constant in the light-adapted state was on average about 4 deg. After dark adaptation it was up to a factor of three larger, with a median ratio of 1.85. Response delays, latencies and durations for (equal amplitude) threshold flash responses substantially increased during dark adaptation. Copyright © 1996 Elsevier Science Ltd

Horizontal cell Dark adaptation Cat retina Spatial and temporal properties

INTRODUCTION

Spatial resolution of cat retinal ganglion (G-) cells declines as background level falls. This may be due to changes in either the spatial characteristics of receptive field centre and surround, or to differential desensitization of centre and surround, or a combination of the two (Shapley & Enroth-Cugell, 1984). G-cell and LGN studies have not provided a complete, consistent account of the relative contribution of these different effects to changes of receptive field organization. Chan *et al.* (1992) and Derrington and Lennie (1982) reported little or no change of centre and surround size throughout the mesopic and scotopic range. Other studies suggested an increase of centre size with falling background illumination (Kaplan *et al.*, 1979; Virsu *et al.*, 1977; Enroth-Cugell & Robson, 1966). Such discrepancies partly arise from difficulties in separating centre and surround sizes and strengths. In a difference of Gaussians model these parameters are inevitably correlated. In this study we addressed the effects of adaptation level on horizontal (H-) cell receptive fields. H-cells presumably are major contributors to G-cell receptive field surrounds and their properties at different adaptation levels thus provide relevant information for understanding the changes in G-cell receptive field organization.

The effects of dark adaptation on H-cell spatial and temporal properties have been extensively investigated in lower vertebrates. The results, however, are species dependent and cannot easily be extrapolated to the mammalian retina. Dong and McReynolds (1992) and Myhr *et al.* (1994), for example, found substantial increases in receptive field size in the mudpuppy whereas, for example, Tornqvist *et al.* (1988) and Mangel and Dowling (1985) found the opposite in teleost fish. To better understand the role of H-cells in the dark-adapted cat retina we therefore studied the effects of prolonged dark adaptation on H-cell sensitivity, their rod and cone inputs and their spatio-temporal properties.

To this end, cat H-cells were recorded in the optically intact, *in vivo* eye. Elsewhere (Lankheet *et al.*, 1996) we showed that H-cell sensitivity only increased by about 2 log units during 45 min of dark adaptation after a photopic adaptation light. We also showed how the observed increase of sensitivity resulted from changes in the rod and cone inputs, and corresponds to a gradual change of the hyperpolarization level (van de Grind *et al.*, 1996). Although threshold responses were rod dominated, H-cell absolute thresholds were in the mesopic range; H-cells remained insensitive in the scotopic range. This finding is consistent with the hypothesis of a H-cell contribution to G-cell surrounds, since it is well established that upon dark adaptation the surround

*Neuroethology, Helmholtz Institute and Comparative Physiology, Universiteit Utrecht, Padualaan 8, 3584 CH Utrecht, The Netherlands.

†To whom all correspondence should be addressed [*Email* lankheet@neuretp.biol.ruu.nl].

mechanism becomes weaker relative to the centre (Barlow *et al.*, 1957; Chan *et al.*, 1992; Enroth-Cugell & Lennie, 1975; Derrington & Lennie, 1982; Kaplan *et al.*, 1979). In this paper we studied the changes of H-cell response properties that occurred with the changes in sensitivity upon dark adaptation. We compare H-cell receptive field size and temporal response parameters in the light-adapted eye, and after prolonged dark adaptation.

METHODS

Preparation and recordings

Horizontal cell activity was recorded *in vivo*, in the optically intact eye. Results were obtained in four adult cats of either sex (body wt between 3.0 and 6.0 kg). Cats were under pentobarbital anaesthesia (Nembutal), which was initiated by an i.p. injection of 40 mg/kg body wt, and were paralysed with gallamine triethiodide (Flaxedil). The trachea was cannulated for artificial respiration. End-tidal [CO_2] was kept near 4.0% by adjusting the respiratory volume. The rectal temperature was kept near 38.0°C. The femoral artery and vein were cannulated for continuous infusion, and for monitoring the intra-aortic blood pressure. All wounds and pressure points (ears) were locally anaesthetized with 2% Lidocaine. Heart rate, blood oxygen saturation level and blood pressure were monitored as additional indicators of the cats' physiological state. Anaesthesia and paralysis were maintained with infusion of a 5% Ringer solution (6 ml/hr) containing 3 mg Nembutal and 6 mg Flaxedil per kg per hr. Atropine and phenylephrine hydrochloride (2%) were applied locally to dilate the pupils and to retract the nictitating membrane. The eye was sewn to a metal ring which was rigidly attached to the stereotaxic device. The contact lenses protecting the cornea had artificial pupils of 1.5×6 mm. Micropipette electrodes were filled with 4 M potassium acetate. Successful electrodes had an impedance of 15–60 MΩ, measured at 1 kHz. Intracellularly recorded membrane potentials were partly analysed on-line, and stored on a digital tape recorder (Bio Logic) for off-line analysis. The pass-band of the tape recorder was from dc to 12 kHz. For on-line analysis the amplified responses were digitized at a sampling frequency of 1 kHz. More details can be found in previous papers (Lankheet *et al.*, 1990, 1991a, b).

Light stimulus

Visual stimuli were generated by two independent optical channels. Each channel had a 450 W xenon light source which was driven by a modulatable power amplifier (Heinzinger). The mean, steady light intensity was controlled by neutral density filters, that allowed attenuation between −6.0 and 0 log units, in steps of 0.1 log units. The maximum intensities were 4.2 log cd/m^2 (spot sizes up to 4.0 deg dia) and 3.25 log cd/m^2 (spot sizes up to 8.8 deg dia). High speed shutters in the light paths were used to generate flashes varying in duration between 10 msec and several seconds. Continuous light intensity modulations were controlled by programmable Wavetek signal generators driving the Heinzinger power amplifiers. The two channels were combined using a half-mirror. A mechanical oscilloscope (Molenaar *et al.*, 1980) projected the spots concentrically on a tangent back projection screen. The screen was at a distance of 57 cm from the cat's eye and subtended 80×80 deg. For the cat eye 1 deg of visual angle corresponds to 218 mm on the retina (Vakkur & Bishop, 1963).

Experimental protocol

The search stimulus was a large (8.8 deg dia) spot that was square-wave modulated in intensity at a frequency of 1 or 2 Hz. The mean luminance was in the photopic range (3.1 log cd/m^2) and the modulation contrast was 0.66. Horizontal cells were identified by their characteristic response properties. Only the most stable recordings with large response amplitudes were used for the dark adaptation experiments. The receptive fields were located within 15 deg distance from the centre of the area centralis (estimated by back projection of the optic disc and retinal blood vessels onto the tangent screen).

Before dark adapting the cell we performed several standard measurements of H-cell spatial, temporal and sensitivity characteristics. H-cell receptive field profiles (RFPs) were measured with spots flashed at different positions across the receptive field. The flash duration was 10 msec and the intensity was adjusted to obtain maximal responses in the range of 5–15 mV. Horizontal and vertical RFPs were measured at two different spatial resolutions (spot size 4.3 deg, 2 deg spacing and spot size 2.3 deg, 0.75 deg spacing). The mean background illumination in the light-adapted condition, and in the absence of a light spot was about −1.0 log cd/m^2. Between different experiments we employed the search stimulus to keep the cell well light adapted and to check the stability of the recording. During and after dark adaptation we took great care to eliminate any background illumination.

Response vs intensity (*R–I*) curves were measured for white light, for green (503 nm) light that was near optimal for rods, and for orange (581 nm) light that was relatively more effective for the dominant cat cone (optimum absorption at 555–560 nm). *R–I* curves were measured with a 4.3 deg dia spot and 200 msec flash duration. Flash intensities were increased in steps of 0.4 log units and the interval between successive flashes was 2 sec. The pre-dark adaptation experiments included several other measurements, the results of which were not used in the present study.

After the initial measurements the cell was light adapted for 10 sec to a large spot with a mean luminance of 3.8 log cd/m^2. The duration of 10 sec was sufficient to fully adapt the cell to this photopic light level, but bleaches insignificant amounts of rhodopsin (Bonds & MacLeod, 1974). Immediately following the 10 sec light adaptation the cell was dark adapted for a duration of 10–45 min. Great care was taken to create total darkness and to prevent any stray light from reaching the eye. After

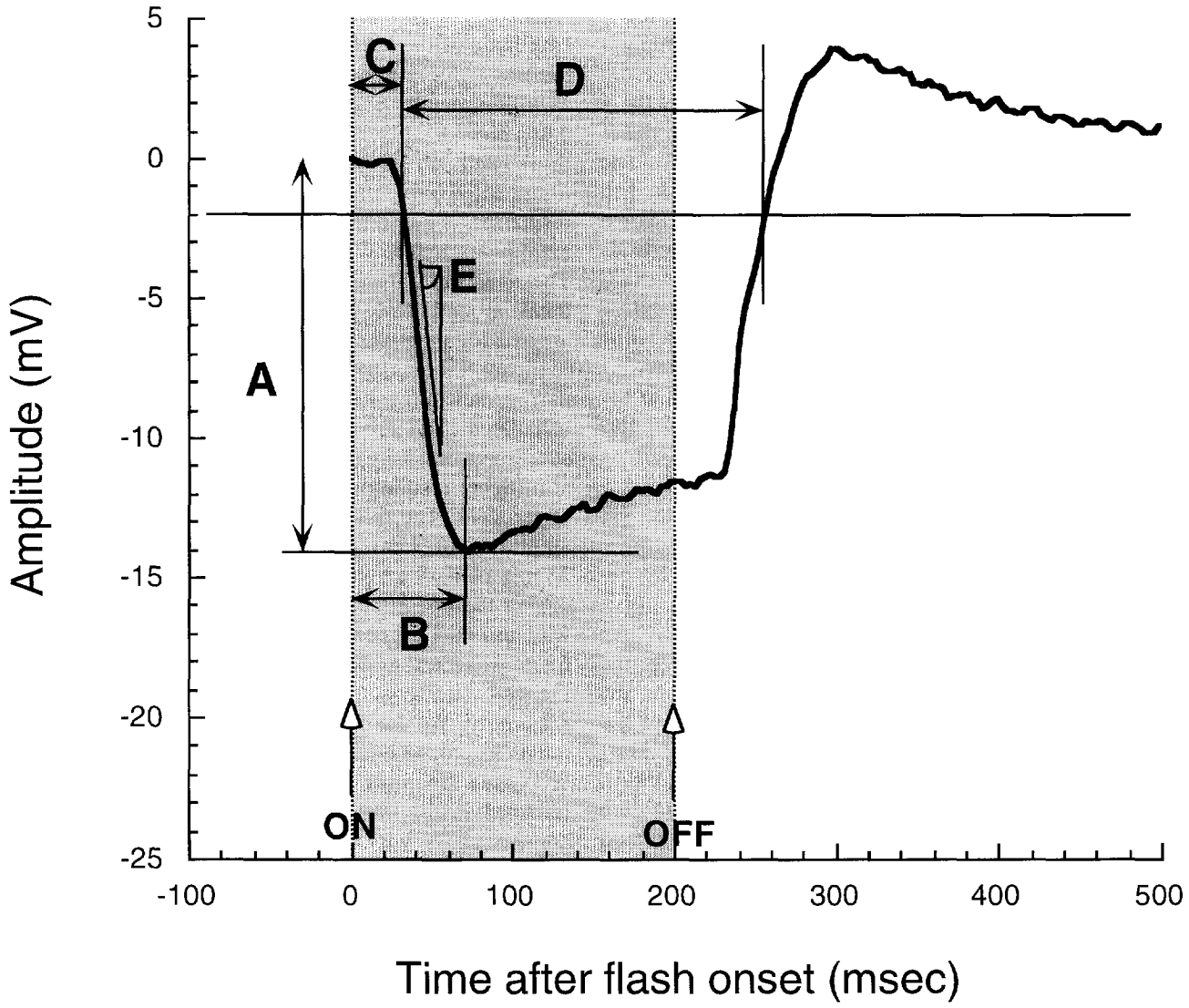

FIGURE 1. Example of an H-cell flash response, and illustration of the response measures we used. (A) Response peak amplitude; (B) peak delay; (C) response latency, measured at a criterion amplitude of 2 mV; (D) duration of the hyperpolarization; (E) maximum slope of the on-response.

dark adaptation, and still in total darkness, we repeated the standard set of measurements that was also performed before dark adaptation. Light intensities were adjusted so as to produce roughly the same response amplitudes as in the light-adapted condition preceding dark adaptation.

During dark adaptation sensitivity was measured at intervals of 1 min, for white light, 503 and 581 nm lights. A 4.3 deg spot was flashed at increasing intensities until a criterion response amplitude was reached. Flash duration was 200 msec and flash intensities were increased in steps of 0.4 log units. The threshold for each test light was automatically tracked and the range of test intensities was adjusted to the last threshold measurement. Testing started at 2.0 log units below the estimated threshold, which resulted in four or five flash intensities for each test light. Subsequent flashes for a single threshold measurement were given at about 2 sec intervals. Elsewhere (Lankheet *et al.*, 1996) we compared the sensitivity curves for the three different test lights to disentangle rod and cone contributions to sensitivity increases. Here we summarize the results for white light only.

Data analysis

Figure 1 shows an example of an H-cell response to a 200 msec test flash, and illustrates the response measures that we used to quantify the amplitude and temporal characteristics. Response peak amplitude (A) and time-to-peak (B) were calculated from the on-line digitized flash responses. Other response parameters were calculated from data saved to disk. Response latency (C) was defined as the time since stimulus onset at which the response exceeded a threshold value of 2 mV. (D) quantifies the duration of the hyperpolarization as the time between the on and off 2 mV threshold crossings. (E) indicates the maximum slope of the on-response. To compress the digitized data for storage on disk, three or four successive samples were averaged. This resulted in a lower temporal resolution (250 or 333 Hz), but higher

signal to noise ratio. The resulting sampling frequency was still high enough to accurately estimate the temporal response parameters.

H-cell spatial properties were quantified with a receptive field model based on passive spread, and linear spatial summation in an extended cable network. The model was originally proposed for the S-space in fish retinae by Naka and Rushton (1967) and has been shown to describe the spatial properties of, for example, turtle H-cells (Lamb, 1976) and cat H-cells (Nelson, 1977; Lankheet *et al.*, 1990). The model quantifies receptive field sizes by a characteristic length constant, λ, the value of which does, in principle, not depend on spot size.

The voltage V as a function of the distance (r) to the centre of the spot is given by the following formulas (Lamb, 1976):

$$V(r) = V_{\max} 1 - \frac{a}{\lambda} K_1\left(\frac{a}{\lambda}\right) I_0\left(\frac{r}{\lambda}\right) \text{ for } r \leq a \quad (1)$$

$$V(r) = V_{\max} \frac{a}{\lambda} I_1\left(\frac{a}{\lambda}\right) K_0\left(\frac{r}{\lambda}\right) \text{ for } r \geq a \quad (2)$$

where a is the radius of the light spot, $V_{\max}$ is the amplitude parameter and I_0, K_0, I_1 and K_1 are the modified Bessel functions. We fitted the model to the response peak amplitudes using the Levenberg Marquardt method as implemented by Press *et al.* (1986). Confidence limits on the optimized length constants were determined by perturbing its value until the mean squared error, obtained after re-optimizing the amplitude parameter (E), had increased by 5% [see Lankheet *et al.* (1990)].

RESULTS

Dark adaptation and H-cell sensitivity

We first describe the change of H-cell sensitivity during dark adaptation. Second, we will compare the spatial and temporal properties as measured before and after dark adaptation.

Figure 2 illustrates the effect of dark adaptation on H-cell response vs intensity characteristics. Figure 2(A) shows the responses to 200 msec flashes in the light-adapted eye. Flash intensities increased in steps of 0.4 log unit, from 0.2 to 4.2 log cd/m^2. The maximum amplitude of about 20 mV was limited by the maximum light intensity in our setup, rather than by response saturation. Both the on and the off response were characterized by a transient overshoot. The rods were presumably fully saturated since no signs of a rod aftereffect (RAE) were observed. Figure 2(B) shows responses to the same flash intensity series, measured after 24 min of dark adaptation. The responses now clearly have a substantial rod component, as can be seen by the presence of a RAE; off-responses to bright flashes show an initial fast depolarization due to cone-input, followed by a delayed return to the base line. The amplitude of the RAE, i.e. the plateau after stimulus offset, indicates the maximum rod contribution to the responses, which for this cell was about 10 mV. The amplitude of the RAE did not depend on the intensity of the test light, nor on the chromaticity (Lankheet *et al.*, 1996). Especially small amplitude responses were slowed down considerably; they show much longer rise and fall times and no signs of on-transients. Off-transients disappeared altogether, for both low and high amplitude responses. Figure 2(C) compares the response peak amplitudes before (○) and after (●) dark adaptation. The *R–I* curve after dark adaptation shows a rod–cone break around 2.5 log cd/m^2. The *R–I* curve shifted by about 2 log units during dark adaptation.

Figure 3 shows the time course of the threshold change during dark adaptation. The threshold intensities were calculated by interpolating between responses for successive intensity steps, and could thus be estimated at a higher resolution than the 0.4 log units steps in the experiment. The threshold, corresponding to a criterion amplitude of 4 mV, declined steadily during the first 35 min of dark adaptation and remained fairly constant during the last 10 min. The total increase in sensitivity was less than 2 log units. Similar results were obtained for other recordings. In our previous paper we analysed the rod and cone contributions to the increase of sensitivity. We found that the increase of the amplitude range for rod-driven activity (release from saturation) accounted for most of the sensitivity increase. This is reflected in the increase of the RAE in Fig. 2. In the present paper we studied the change of spatial and temporal properties that accompanied these threshold changes.

Receptive field size

Figure 4 shows a representative example of RFPs measured in the light-adapted state [Fig. 4(A and C)], and after 24 min of dark adaptation [Fig. 4(B and D)]. The profiles on the left-hand side were obtained with horizontal spot displacements, the ones on the right-hand side with vertical displacements. Figure 4(A and B) show the results for a spot diameter of 4.3 deg at 2.0 deg intervals, Fig. 4(C and D) for a spot size of 2.3 deg displaced in steps of 0.75 deg. It can be seen that dark adaptation has a marked effect on both spatial and temporal H-cell properties. The impulse responses were much slower after dark adaptation and the receptive fields became substantially larger. To quantify the size of the receptive fields we applied a receptive field model based on passive electrical spread and linear spatial summation in a coupled H-cell network (see Methods). Figure 5 shows an example of response peak amplitudes (●), together with the best fitting profiles based on equations (1) and (2). The stimulus parameters for the different panels were equal to those for the corresponding panels in Fig. 4. The model fitted the measured profiles fairly accurately, and significantly better than a simple, Gaussian shaped profile. The numbers in the upper right corner give the length constant for each profile. Different spot sizes and horizontal and vertical displacements yielded roughly the same estimates for the length

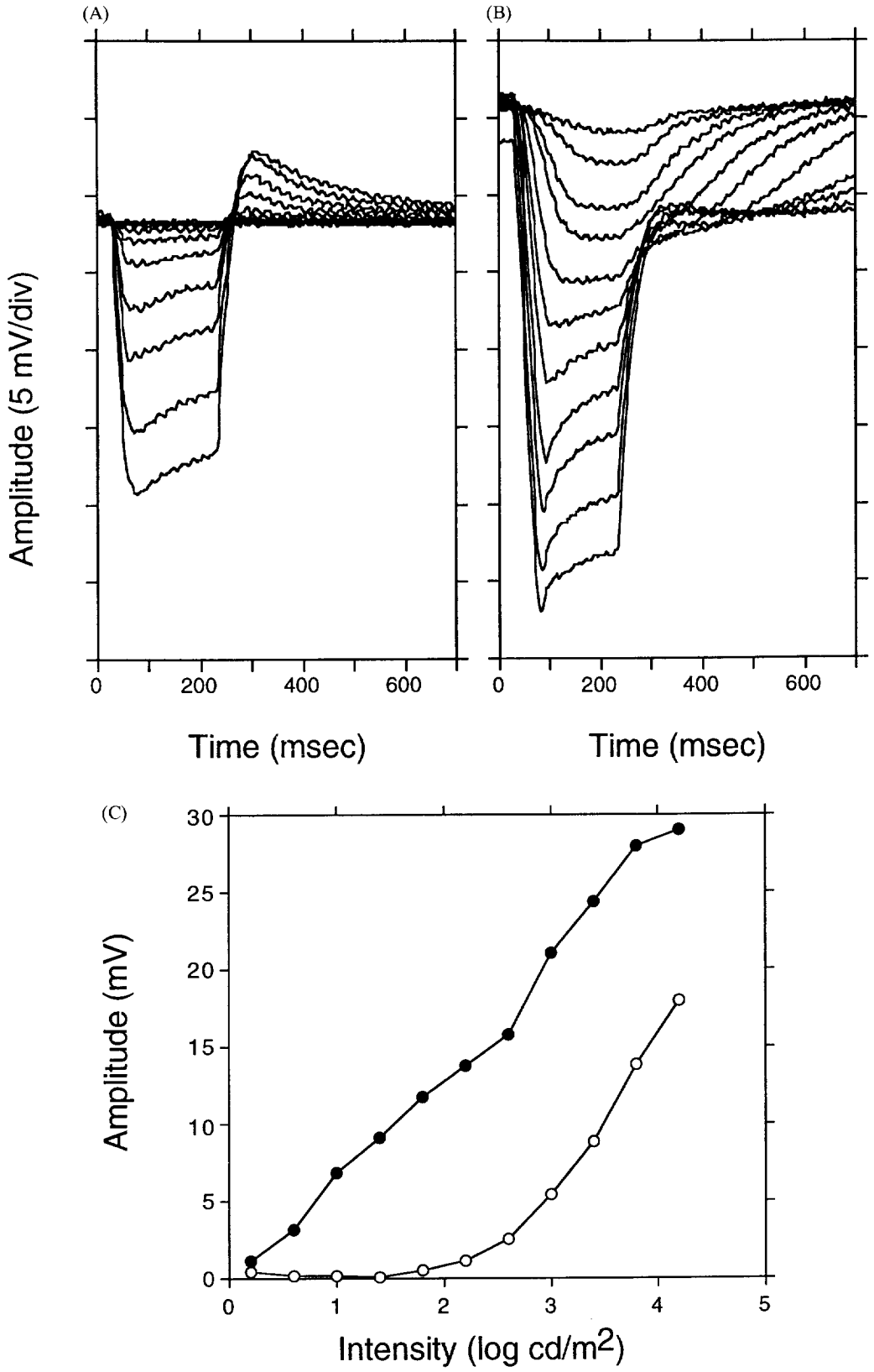

FIGURE 2. The effect of dark adaptation on H-cell response vs intensity characteristics. (A) and (B) show responses to the same flash intensity series in the light-adapted and dark-adapted eye, respectively. The time is given relative to flash onset. Flash duration was 200 msec. Flash intensities increased in steps of 0.4 log unit, from 0.2 to 4.2 log cd/m^2. Cell 94-1, dark adapted for 24 min. (C) Shows the peak amplitudes for the responses in A (○) and B (●).

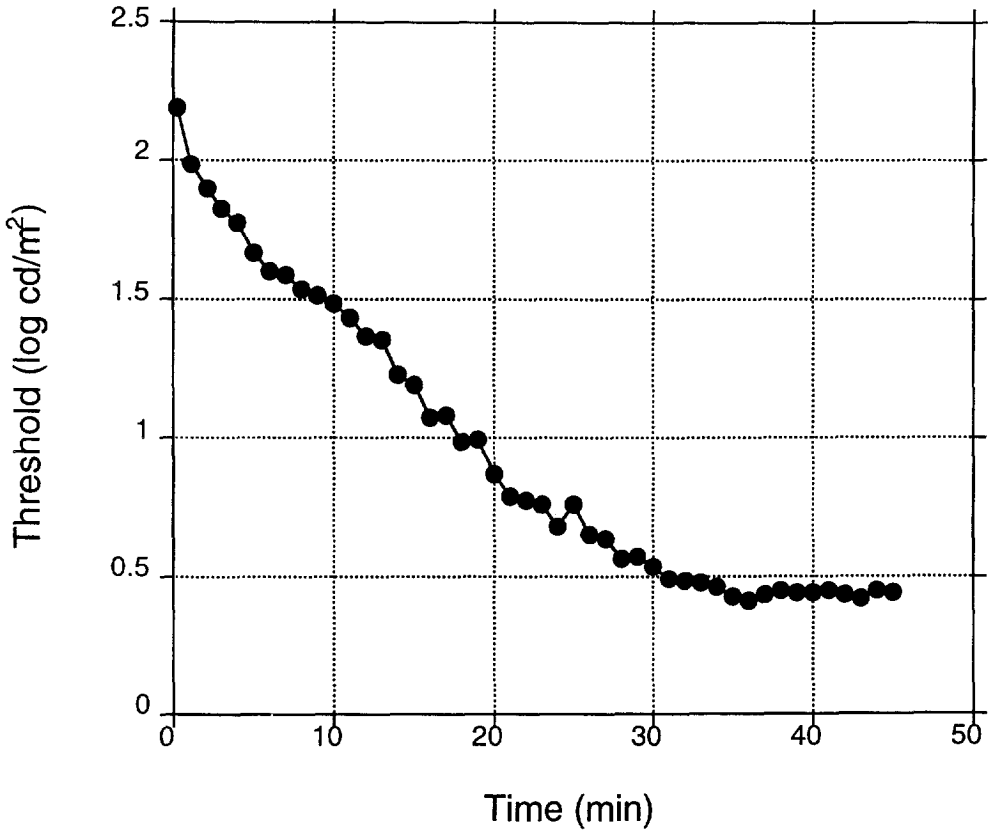

FIGURE 3. Horizontal cell threshold for white light during prolonged dark adaptation. Thresholds were assessed at 1 min intervals by increasing the intensity in steps of 0.4 log units until a criterion response was reached. The thresholds were calculated for a threshold amplitude of 4 mV, by interpolating between amplitudes for sub- and supra-threshold responses. Cell 94-2.

constant. However, the length constants for the light-adapted and for the dark-adapted profiles differed substantially. In the light-adapted state the mean λ value for this cell was 3.6 deg, whereas after dark adaptation it was 7.8 deg.

Comparable results were obtained for other recordings. For 12 cells that were dark adapted for at least 10 min we were able to measure RFPs before and after dark adaptation. Figure 6(A) compares the length constants before and after dark adaptation. Before dark adaptation the length constant was about 3–5 deg (median 4.6 deg). After dark adaptation the receptive field sizes were more variable, but they were consistently larger. The increase in receptive field size (mean value for different spot sizes and for horizontal and vertical) ranged from a factor of 1.05 to 3.66 for different cells. On average, the length constant was a factor of 1.98 (SD 0.83) larger in the dark-adapted state. The median value was 1.85, indicating that the effect was not due to a few outliers. Part of the variability may be due to differences in the duration of dark adaptation (10–45 min). However, within our limited sample of H-cells we found no clear correlation between the duration of adaptation for a cell and the effect on receptive field size. This might indicate that the increase in receptive field size has a faster time course than the sensitization itself. Such an explanation is consistent with the finding of Brown and Murakami (1968) that effects of light and dark adaptation on receptive field organization of cat S-potentials are faster than the time course of sensitization.

Temporal properties

The impulse responses in Fig. 4 also demonstrated a pronounced effect of dark adaptation on H-cell temporal properties. This is shown more clearly in Fig. 7, which presents the response to a single, 10 msec, test flash, centred on the receptive field, in the light-adapted state. A similar response measured after 25 min of dark adaptation is shown superimposed. In the dark-adapted state the flash intensity was reduced to obtain a response of roughly the same amplitude. In the light-adapted state the response reached its maximum in about 60 msec, and the total response lasted about 100 msec. After dark adaptation both the peak delay and the response duration have substantially increased.

In Fig. 6(B) we compare the peak delays for a centred, 10 msec, flash in the light-adapted state and in the dark-adapted state. Before dark adaptation the peak delays ranged from 50–80 msec, for both spot sizes (mean 63 msec, SD 5.4 msec). After dark adaptation the delays were more variable (70–120 msec), but always significantly larger (mean 94 msec, SD 13.4 msec). On average the peak delays increased by a factor of 1.5.

Similar changes of response dynamics could be

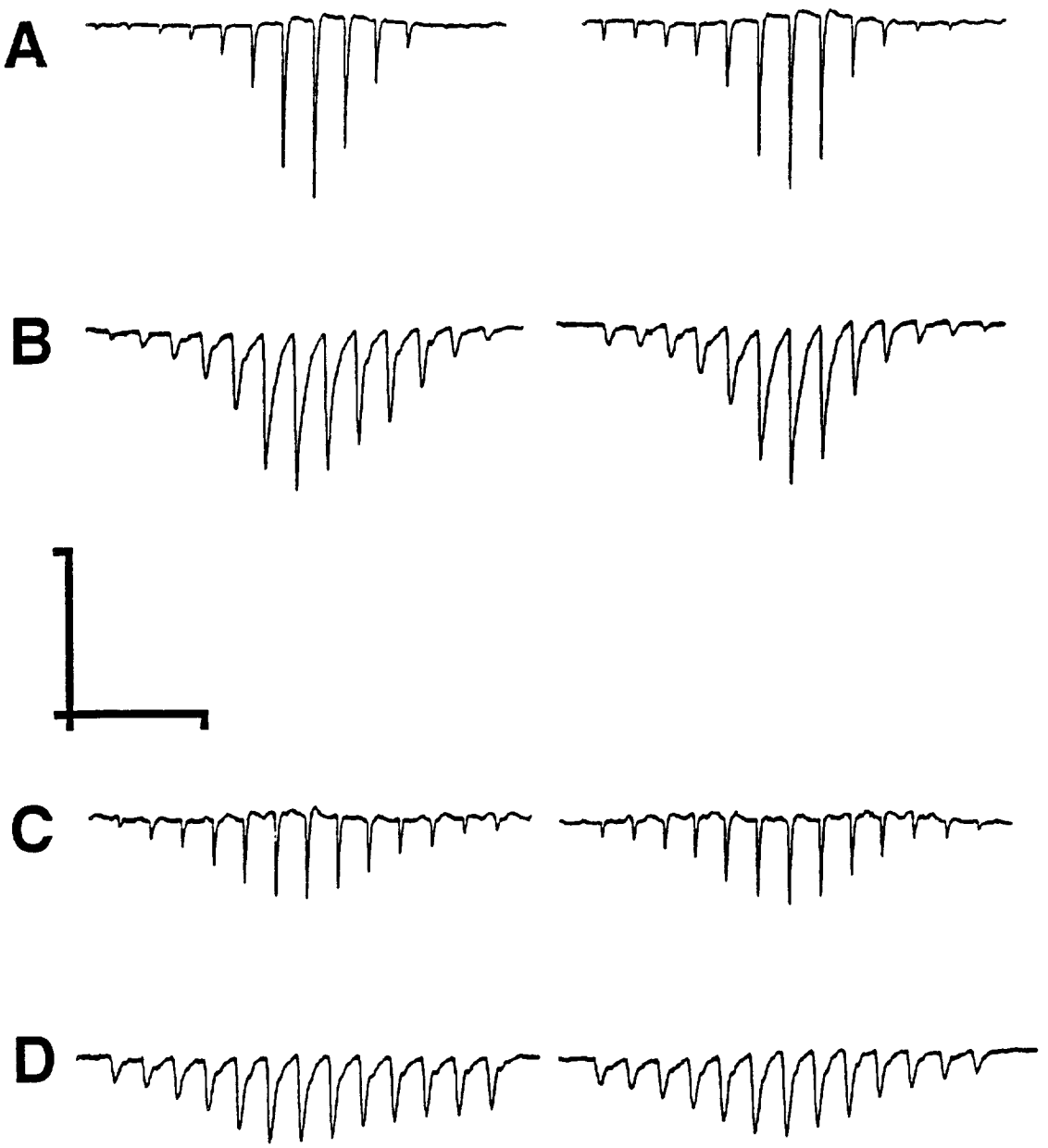

FIGURE 4. Comparison of receptive field profile measurements in the light-adapted (A and C) and in the dark-adapted eye (B and D). (A and B) show results for a 4.3 deg diameter spot, flashed (10 msec) at 2 deg spatial intervals; (C and D) are for a 2.3 deg dia spot, at 0.75 deg intervals. Amplitude calibration: 8 mV, time calibration: 2 sec. Cell 94-1, dark adapted for 24 min.

observed for the threshold responses in the course of dark adaptation. In Fig. 8 we show the effect of dark adaptation on several temporal response parameters. Data are presented for the two most stable recordings, in which we dark adapted the cells for 21 and 45 min. The flash responses in Fig. 2(B) show that the response dynamics strongly depend on response amplitude. The dynamics became much faster with increasing amplitude, as can be seen by the shortening of the peak delay, reduction of response latency and increase of the slope. Therefore, we included only threshold responses of similar amplitude (4–6.5 mV); responses of lower, or higher amplitude were discarded. In this way, differences in temporal properties were minimally confounded with differences in response amplitude. Figure 8(A) shows a gradual increase of the time-to-peak during dark adaptation. It increased from about 80 msec immediately after light adaptation to over 200 msec (i.e. the flash duration) after prolonged dark adaptation. Figure 8(B) shows the latencies for the same responses, measured at a threshold criterion of 2 mV. Latencies increased from about 35 msec immediately after light adaptation to about 90 msec after completion of dark adaptation. The maximum slope of the on-hyperpolarization decreased by about a factor of two during dark adaptation. The slope reached a minimum of 0.08 mV/msec at the end of dark

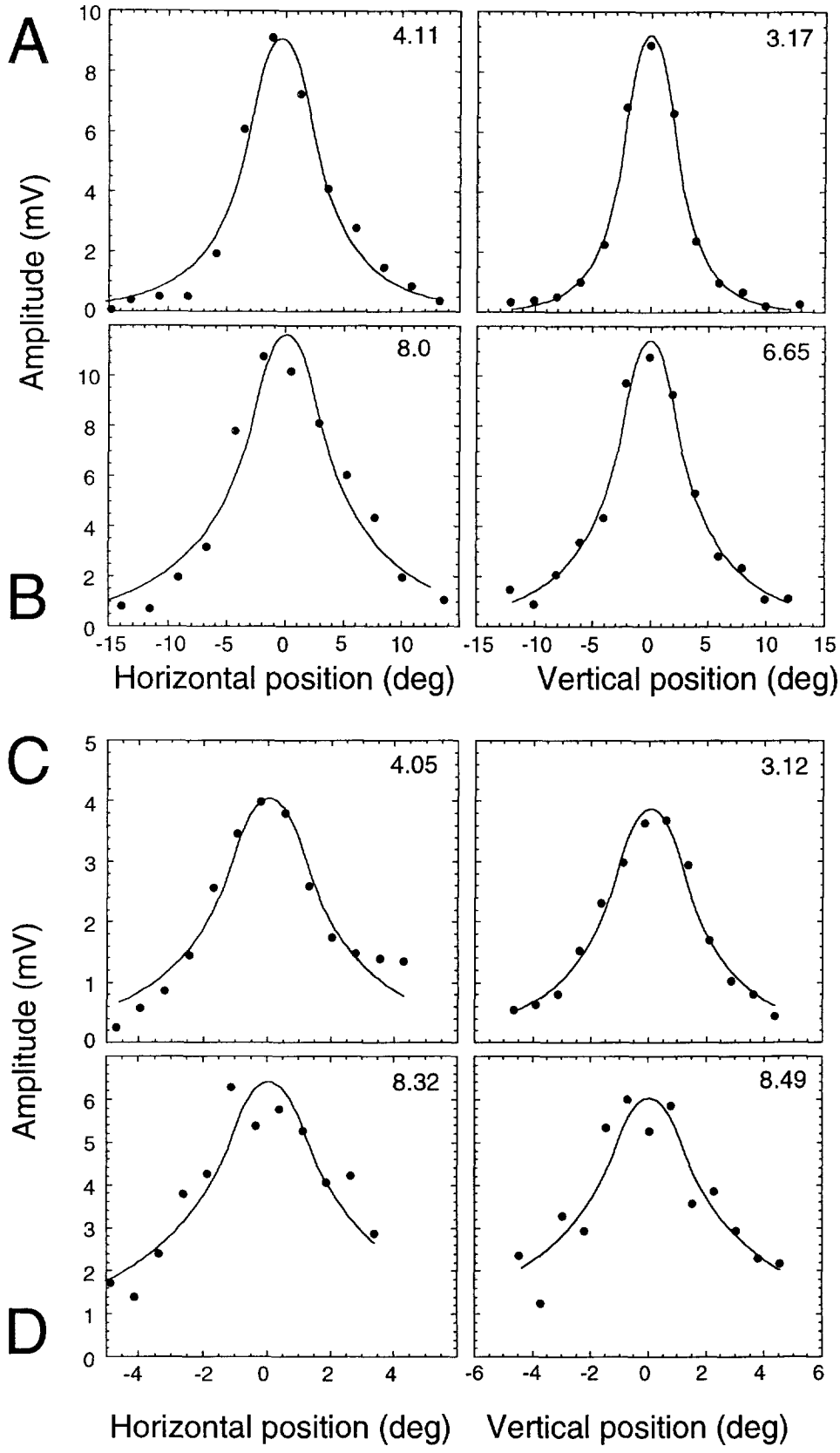

FIGURE 5. Receptive field profiles measured before and after dark adaptation. Symbols represent peak amplitudes for responses as shown in Fig. 4. Stimulus parameters for the different panels were similar to those in Fig. 4. The solid lines are fits based on equations (1) and (2). The optimized length constant is given in the upper right corner of each panel. Cell 94-1, dark adapted for 22 min. This is the same recording as in Fig. 4, but the data were obtained in a second dark adaptation cycle.

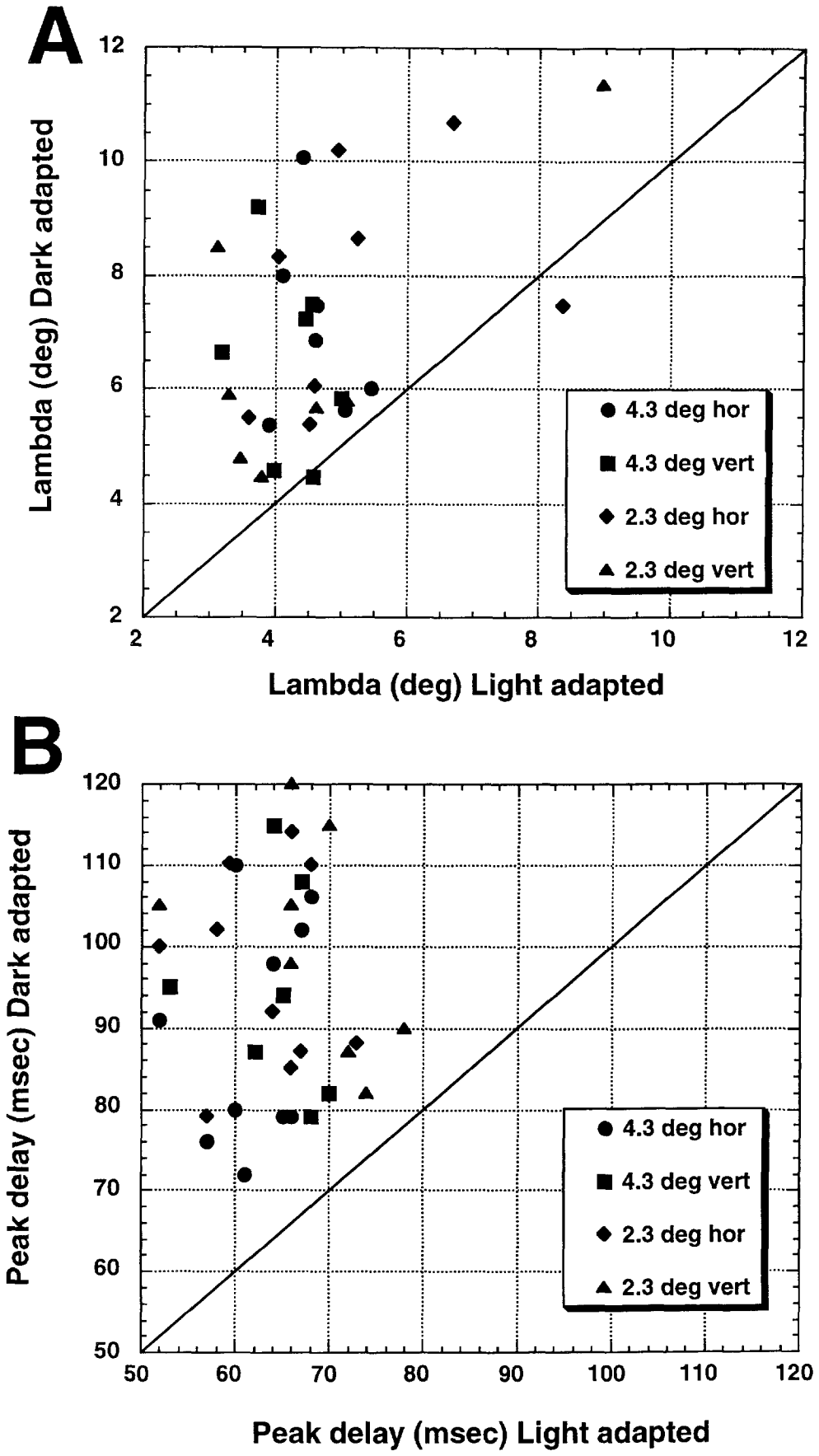

FIGURE 6. A comparison of spatial and temporal response properties before and after dark adaptation. (A) Shows the length constant after dark adaptation plotted vs the value in the light-adapted state; (B) shows the peak delays after dark adaptation plotted vs the delay before dark adaptation, for responses to a centred 10 msec test flash. Data for 12 cells that were dark adapted for a duration of 10–45 min. Different symbols represent results for different spot sizes and horizontal and vertical displacements (see inset).

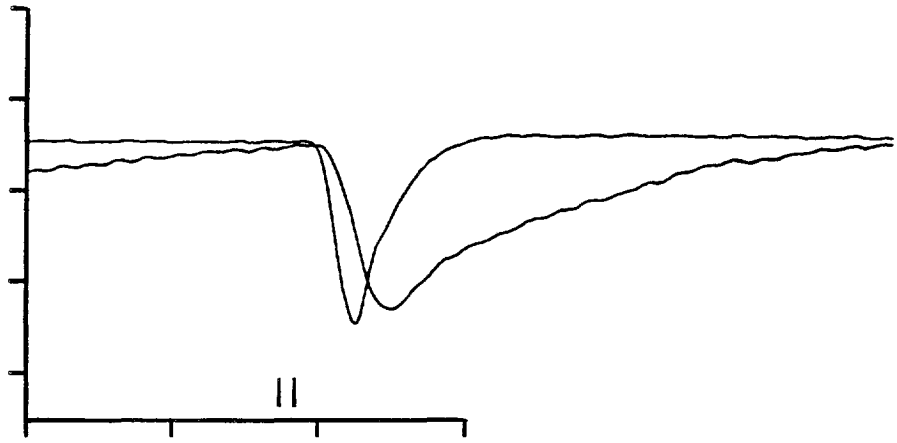

FIGURE 7. Impulse responses before and after dark adaptation. Responses to 10 msec flashes of a centred, 4.3 deg dia, test spot are superimposed on one another. The vertical lines indicate the on and offset of the test flashes. Cell 94-1. Amplitude calibration 4 mV/div.; time calibration 100 msec/div.

adaptation. The effects of dark adaptation on the off-response were even larger, which resulted in an increase of the response duration by about 80 msec.

DISCUSSION

In this paper we described H-cell spatial and temporal response properties after prolonged dark adaptation. It should be noted, though, that H-cell sensitivity never reached the threshold levels of dark-adapted G-cells. Threshold stimuli for H-cells were always several log units above the absolute threshold in G-cells. The sensitization in H-cells amounted to about 2 log units maximally. The increase of receptive field size and decrease of temporal resolution suggests that this sensitization is, at least partly, due to a larger summation area, and to more extensive temporal integration.

Response latencies, peak delays and maximum slopes all increased by roughly a factor of two during prolonged dark adaptation. The change of response dynamics probably resulted from the gradual change from pure cone responses to rod dominated responses (Lankheet *et al.*, 1996), as well as from the slowing down of rod responses during dark adaptation. Our results showed a clear and substantial effect of dark adaptation on H-cell spatial properties. H-cell receptive fields increased by a factor of 1.85 (median). This effect is surprisingly large, given the low background light level (-1 log cd/m^2) on which we measured the "light-adapted" profiles. This background illumination level is in the mesopic range, suggesting that most of the difference in receptive field size (relative to the dark-adapted state) must have resulted from (long-) lasting effects of the photopic search/adaptation stimulus. Measured on photopic backgrounds the receptive fields presumably would have been even smaller. Also, some of these effects were obtained with dark-adaptation durations as short as 10 min, whereas the sensitization due to dark adaptation continued for about 35 min. Thus, many of the cells were not fully dark adapted. The described effects of dark adaptation on spatial and temporal properties should therefore be regarded as minimal estimates.

The change of receptive field size was based on optimized length constants for a leaky cable-network model (Naka & Rushton, 1967; Lamb, 1976). Since both receptive field size and sensitivity were free parameters in the model fit, the estimated length constant was minimally affected by changes of sensitivity. In addition, to discount sensitivity differences as much as possible we adjusted the intensities to obtain equal amplitude responses. Inspection of the profiles in Fig. 5 shows that a different measure for the receptive field size might have yielded different results. The width at half height was relatively less affected by dark adaptation. Such a measure, however, ignores the full characteristic shape of the profiles, and is therefore a less suitable descriptor of the underlying spatial summation properties. The same holds for applying Gaussian profiles. H-cell RFPS were generally not very well described by Gaussians. The tails of a Gaussian profile typically fall off too steeply. Both the width at half height and a Gaussian profile would yield different estimates for the size of the receptive field for different spot sizes. The model on the other hand, yields similar values for different spot sizes, and therefore seems to account for both the spatial summation and spatial spread of local signals, both of which determine the shape of the profiles measured with circular spots.

In the dark-adapted retina, the H-cell responses were mainly rod driven. The change of receptive field size might thus also result from a change from cone input to rod input. Rod signals reach the horizontal cells through cones, which sum the input from surrounding rods. A shift from cone to rod driven H-cell responses may thus also reflect more extensive spatial summation within the rod–cone network. However, since in the cat retina the rods are not interconnected, this effect is expected not to

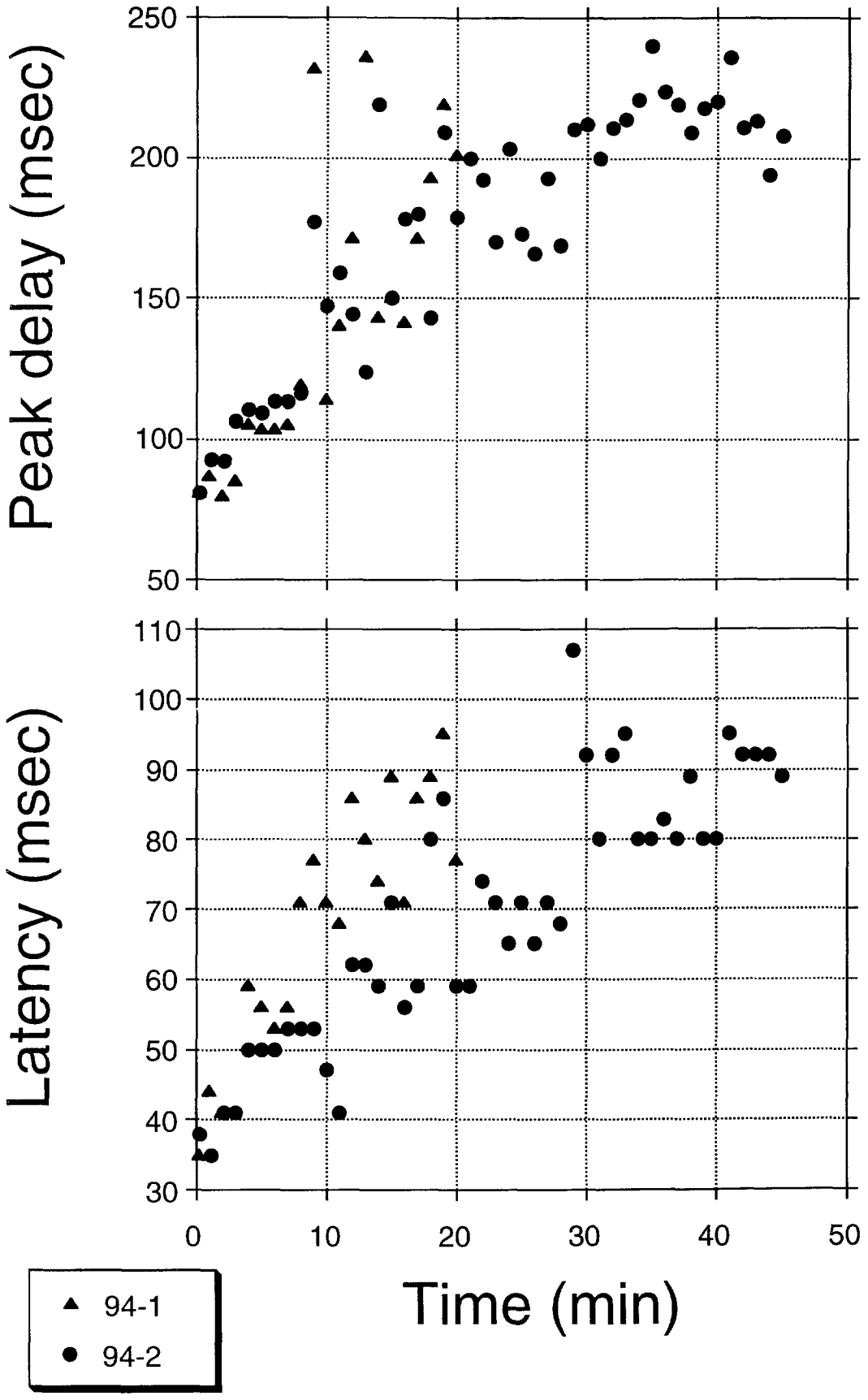

FIGURE 8. Change of response dynamics during dark adaptation. Shown are several temporal response parameters for threshold responses of about 4 mV, for 200 msec white flashes of a 4.3 deg dia spot. The response measures are illustrated in Fig. 1.

exceed the rod–cone distance and is, therefore, insignificantly small (Chan *et al.*, 1992).

Although there is an extensive literature on similar and related findings for H-cells in lower vertebrates, our data do not allow us to pinpoint the cause of the observed changes in receptive field size. The effect could result from increased coupling in either the receptor layer, or the H-cell layer, for example due to opening of gap junctions. Modulation of electrical coupling between horizontal cells by prolonged darkness and background illumination has been shown for cone-driven horizontal cells in many lower vertebrates (Witkovsky & Dearry, 1992). Similar, dopamine mediated, mechanisms might play a role in the cat retina. However, given the diversity of findings among fish, turtle etc, a direct comparison of results for mammalian H-cells to those of lower vertebrates seems less relevant. Our data especially differ from findings for fish retinae, because they are often complicated by effects of dark suppression and light sensitization. In the white perch retina, for example background illumination is needed to maintain extensive electrical coupling between H-cells (Yang *et al.*, 1988a, b; Yang *et al.*, 1994; Tornqvist *et al.*, 1988). Similar effects have been reported for other fish retinae (Mangel & Dowling, 1985; Mangel *et al.*, 1994). Yang and coworkers suggested that this might be a general phenomenon, which could explain the absence of G-cell surrounds after prolonged dark adaptation. We found, however, no signs of either dark suppression or light sensitization in cat H-cells. On the contrary, cat H-cells were always most sensitive after prolonged dark adaptation, although their absolute sensitivity remained relatively low.

As mentioned in the introduction, G-cell studies have not provided a consistent account of the effect of dark adaptation on G-cell receptive field organization. If H-cells form the surround mechanisms we should expect an increase in surround size, in going from photopic to low mesopic light levels. Although some studies indicated an increase of surround size [e.g. Barlow *et al.* (1957); Enroth-Cugell & Robson (1966)] this is generally not found. Fitting a centre–surround model to their data, Chan *et al.* (1992) and Derrington and Lennie (1982) found no, or insignificantly small changes in centre and surround size. We also applied Gaussian profiles (not shown) and found that our H-cell profiles were not well described by Gaussians, and that the change in receptive field size was generally less impressive if we compared the widths of fitted Gaussians. We conclude therefore that H-cell receptive fields do increase during dark adaptation but that these changes might be difficult to confirm at the G-cell level.

REFERENCES

Barlow, H. B., Fitzhugh, R. & Kuffler, S. W. (1957). Change of organisation in the receptive field of the cat's retina during dark adaptation. *Journal of Physiology, 137*, 338–354.

Bonds, A. B. & MacLeod, D. I. A. (1974). The bleaching and regeneration of rhodopsin in the cat. *Journal of Physiology, 242*, 237–253.

Brown, K. T. & Murakami, M. (1968). Rapid effects of light and dark adaptation upon the receptive field organisation of S-potentials and late receptor potentials. *Vision Research, 8*, 1145–1171.

Chan, L. P., Freeman, A. W. & Cleland, B. G. (1992). The rod–cone shift and its effect on G-cells in the cat's retina. *Vision Research, 32*, 2209–2219.

Derrington, A. M. & Lennie, P. (1982). The influence of temporal frequency and adaptation level on receptive field organisation retinal ganglion cells in cat. *Journal of Physiology, 333*, 343–366.

Dong, C. J. & McReynolds, J. S. (1992). Comparison of the effects of flickering and steady light on dopamine release and horizontal cell coupling in the mudpuppy retina. *Journal of Neurophysiology, 67*, 364–372.

Enroth-Cugell, C. & Lennie, P. (1975). The control of retinal ganglion cell discharge by receptive field surrounds. *Journal of Physiology, 247*, 551–578.

Enroth-Cugell, C. & Robson, J. G. (1966). The contrast sensitivity of retinal ganglion cells of the cat. *Journal of Physiology, 187*, 517–552.

van de Grind, W. A., Lankheet, M. J. M., Wezel, R. J. A., Rowe, M. H. & Hulleman, J. (1996). Gain control and hyperpolarisation level in cat horizontal cells as a function of light and dark adaptation. *Vision Research, 36*, 3969–3985.

Kaplan, E., Marcus, S. & So, Y. T. (1979). Effects of dark adaptation on spatial and temporal properties on receptive fields in cat lateral geniculate nucleus. *Journal of Physiology, 294*, 561–580.

Lamb, T. D. (1976). Spatial properties of horizontal cell responses in the turtle retina. *Journal of Physiology, 263*, 239–255.

Lankheet, M. J. M., Frens, M. A. & van de Grind, W. A. (1990). Spatial vision properties of horizontal cell responses in the cat retina. *Vision Research, 30*, 1257–1275.

Lankheet, M. J. M., Rowe, M. H., van Wezel, R. J. A. & van de Grind, W. A. (1996). Horizontal cell sensitivity in the cat retina during prolonged dark adaptation. *Visual Neuroscience*, in press.

Lankheet, M. J. M., van Wezel, R. J. A. & van de Grind, W. A. (1991a). Effects of background illumination on cat horizontal cell responses. *Vision Research, 31*, 919–932.

Lankheet, M. J. M., van Wezel, R. J. A. & van de Grind, W. A. (1991b). Light adaptation and frequency transfer properties of cat horizontal cells. *Vision Research, 31*, 1129–1142.

Mangel, S. C., Baldridge, W. H., Weiler, R. & Dowling, J. E. (1994). Threshold and chromatic sensitivity changes in fish cone horizontal cells following prolonged darkness. *Brain Research, 659*, 55–61.

Mangel, S. C. & Dowling, J. E. (1985). Responsiveness and receptive field size of carp horizontal cells are reduced by prolonged darkness and dopamine. *Science, 229*, 1107–1109.

Molenaar, J., Voorhorst, R., Schreurs, A. W., Broekhuyzen, P., Nivard, J. & van de Grind, W. A. (1980). A mechanical oscilloscope for vision research. *Pflügers Archives, 383*, 173–179.

Myhr, K. L., Dong, J. C. & McReynolds, J. S. (1994). Cones contribute to light-evoked, dopamine-mediated uncoupling of horizontal cells in the mudpuppy retina. *Journal of Neurophysiology, 72*, 56–62.

Naka, K. I. & Rushton, W. A. H. (1967). The generation and spread of S-potentials in fish (Cyprinidae). *Journal of Physiology, 192*, 437–461.

Nelson, R. (1977). Cat cones have rod input: A comparison of the response properties of cones and horizontal cell bodies in the retina of the cat. *Journal of Comparative Physiology, 172*, 109–136.

Press, W. H., Flannery, B. P., Teukolsky, S. A. & Vetterling, W. T. (1986). *Numerical recipes: The art of scientific computing*. Cambridge: Cambridge University Press.

Shapley, R. M. & Enroth-Cugell, C. (1984). Visual adaptation and retinal gain controls. *Progress in Retinal Research, 3*, 263–346.

Tornqvist, K., Yang, K. L. & Dowling, J. E. (1988). Modulation of cone horizontal cell activity in the teleost fish retina. III. Effects of prolonged darkness and dopamine on electrical coupling between horizontal cells. *Journal of Neuroscience, 8*, 2279–2288.

Vakkur, G. J. & Bishop, P. O. (1963). The schematic eye in the cat. *Vision Research, 3*, 357–381.

Virsu, V., Lee, B. B. & Creutzfeldt, O. D. (1977). Dark adaptation and

receptive field organisation of cells in the cat lateral geniculate nucleus. *Experimental Brain Research, 27*, 35–50.

Witkovsky, P. & Dearry, A. (1992). Functional roles of dopamine in the vertebrate retina. *Progress in Retinal Research, 11*, 247–292.

Yang, X. L., Fan, T. X. & Shen, W. (1994). Effects of prolonged darkness on light responsiveness and spectral sensitivity of cone horizontal cells in carp retina *in vivo*. *Journal of Neuroscience, 14*, 326–334.

Yang, X. L., Tornquist, K. & Dowling, J. E. (1988a). Modulation of cone horizontal cell activity in the teleost fish retina. I. Effects of prolonged darkness and background illumination on light responsiveness. *Journal of Neuroscience, 8*, 2259–2268.

Yang, X. L., Tornquist, K. & Dowling, J. E. (1988b). Modulation of cone horizontal cell activity in the teleost fish retina. II. Role of interplexiform cells and dopamine in regulating light responsiveness. *Journal of Neuroscience, 8*, 2269–2278.

Yang, X. L. & Wu, S. M. (1989). Modulation of rod–cone coupling by light. *Science, 244*, 352–354.

Acknowledgement—This work was supported by the Life Sciences Foundation (SLW) of the Netherlands Organisation for Scientific Research (NWO).